Original Article

DOI: 10.5582/bst.2021.01017

Role of circulating tumor cell detection in differentiating tumor recurrence from treatment necrosis of brain gliomas

Faliang Gao[1,2,3,§], Wenyan Zhao[4,§], Mingxiao Li[2,3], Xiaohui Ren[2,3], Haihui Jiang[2,3], Yong Cui[2,3], Song Lin[2,3,*]

[1] Department of Neurosurgery, Zhejiang Provincial People's Hospital, People's Hospital of Hangzhou Medical College, Hangzhou, China; Key Laboratory of Endocrine Gland Diseases of Zhejiang Province, China.
[2] Department of Neurosurgery, Beijing Tiantan Hospital, Capital Medical University, Beijing, China;
[3] China National Clinical Research Center for Neurological Diseases, Beijing, China;
[4] General Practice Department, Zhejiang Provincial People's Hospital, People's Hospital of Hangzhou Medical College, Hangzhou, Zhejiang, China.

SUMMARY Differentiating treatment necrosis from tumor recurrence poses a diagnostic conundrum for many clinicians in neuro-oncology. To investigate the potential role of circulating tumor cells (CTCs) detection in differentiating tumor recurrence and treatment necrosis in brain gliomas, we retrospectively analyzed the data of 22 consecutive patients with tumor totally removed and new enhancing mass lesion(s) showed on MRI after initial radiotherapy. The 22 patients were finally classified into tumor recurrence group (n = 10) and treatment necrosis group (n = 12), according to evidence from the clinical course (n = 11) and histological confirmation (n = 11). All 22 patients received CTCs detection, and DSC-MRP and 11C-MET-PET were performed on 20 patients (90.9%) and 17patients (77.3%) respectively. The data of the diagnosis efficacy to differentiate the two lesions by CTC detection, MPR and PET were analyzed by ROC analysis. The mean CTCs counts were significantly higher in the tumor recurrence group (6.10 ± 3.28) compared to the treatment necrosis group (1.08 ± 2.54, $p < 0.001$). The ROC curve showed that an optimized cell count threshold of 2 had 100% sensitivity and 91.2% specificity with AUC = 0.933 to declare tumor recurrence. The diagnostic efficacy of CTC detection was superior to rCBV of DSC-MRP and $rSUV_{max}$ in MET-PET. Furthermore, we observed that CTCs detection could have a potential role in predicting tumor recurrence in one patient. Our research results preliminarily showed the potential value of CTC detection in differentiating treatment necrosis from tumor recurrence in brain gliomas, and is worthy of further confirmation with large samples involved.

Keywords glioma, circulating tumor cell, tumor recurrence, treatment response, radionecrosis

1. Introduction

The current treatment regimen for patients with brain gliomas includes a combination of maximal safe tumor resection, radiation therapy, and chemotherapy after surgery (*1*). This combinatory therapy has prolonged patient life spans, but the increasing use of radiation therapy carries the risk of side effects on the surrounding tissues, resulting in radiation necrosis, while the adjuvant use of temozolomide can exacerbate this side effect (*2*). This treatment response, named "treatment necrosis", is difficult to differentiate from tumor recurrence, as these two outcomes often manifest with similar clinical symptoms and image appearance that characterizes a new contrast-enhancing lesion appearing on a patient's follow-up imaging (*3*). Furthermore, it has also been found that a new contrast-enhancing lesion observed *via* imaging is neither solely necrotic tissue or tumor, but rather a mixture of both lesions, which adds to the complexity of lesion determination (*4*). Given that the treatment for these two lesions differs significantly from one another, differentiating treatment necrosis from tumor recurrence poses a diagnostic conundrum for many clinicians in neuro-oncology.

To date, histological confirmation by biopsy or surgical resection is still the most reliable approach for differentiating treatment necrosis from tumor recurrence. However, both methods are expensive and invasive, and pose an unnecessary risk that negatively impacts patients' lives (*5*). Currently, an increased interest has arisen in development of numerous noninvasive functional imaging modalities, such as Diffusion-

weighted Imaging (DWI), MRI resonance Spectroscopy (MRS), MRP, PET, single-photon emission computed tomography (SPECT) and CT perfusion (CTP), to help differentiate these two lesions (*6*); however, the diagnosis efficiency is not perfect. According to a systematic review study, the diagnostic sensitivity for the two most commonly used imaging modalities, DSC-MRP and 11C-MET-PET, is 79.8% and 76.8% respectively, with a diagnostic specificity of 76.8% and 82.4% respectively (*6*). It is also reported that even with the same imaging modality, the results are not always consistent (*7*). Unfortunately, a noninvasive and reliable method with high diagnostic specificity and sensitivity to distinguish these two lesions is still unavailable.

In recent years, as a major component of "liquid biopsies", circulating tumor cell (CTC) detection has been applied in monitoring treatment response in diverse types of solid tumors (*8-10*), but its application in brain glioma monitoring systems is quite limited. This was mainly due to the traditional concept that CTCs most originally came from the primary tumor and then reached the vascular compartment, but the specific brain environment prevented glioma cells from descending into the blood (*11*). However, this misconception has been corrected by several studies in the past three years. By using different CTCs detection approaches, researchers have successfully identified CTCs in high-grade brain gliomas (*12-14*). Furthermore, in our previous study we demonstrated that CTCs could be detected in all seven common pathological subtypes of brain gliomas, and to some extent, showed its superiority to rCBV of MRP in differentiating treatment necrosis from tumor recurrence in five patients (*15*). The previous studies have given us greater interest in CTC application in differentiating these two lesions, and we postulated that CTCs detection could provide a new perspective towards the diagnosis of treatment necrosis and tumor recurrence in brain gliomas.

In this regard, for the present study, a series of 22 patients with tumor totally removed and afflicted with new enhancing lesions formed after radiotherapy (combined with or without temozolomide) on conventional-contrast MRI imaging were enrolled. Data of CTCs count, rCBV of DSC-MRP and $rSUV_{max}$ of 11C-MET-PET before treatment planning were collected and the diagnosis efficacy of CTC, DSC-MPR and 11C-MET-PET to differentiate treatment necrosis from tumor recurrence were compared by receiver operating characteristic (ROC) analysis. To our knowledge, this is one of the few systematic studies to evaluate the application value of CTC detection and traditional imaging in distinguishing radiation necrosis from tumor recurrence in brain gliomas.

2. Materials and Methods

2.1. Patients and ethics

To perform this study, a series of consecutive patients were retrospectively screened to be included in our study based on all the following criteria: *i*) histologically proven primary brain glioma at first presentation, prior gross total resection of tumor, and prior treatment with radiotherapy, with or without concurrent and adjuvant temozolomide treatment; *ii*) suspicion of new tumor recurrence or treatment necrosis having a new enhancing mass lesion(s) on the initial post-radiotherapy MRI as compared to the pre- radiotherapy MRI; *iii*) proof of tumor recurrence on the basis of direct histology (presence of as any amount of tumor), and proof of treatment necrosis on the basis of either direct histology (complete absence of tumor) or stability of imaging (substantial regression or stability of the enhancing lesions on serial follow-up MRI scans without additional treatment for at least 4 months) (*16,17*), and *iv*) all patients received CTCs detection, and at least one functional imaging modality (DSC-MRP or 11C-MET-PET) before the operation, biopsy or arranged next follow-up period; the interval between CTCs detection, DSC-MRP and 11C-MET-PET exams was within 30 days.

A total of 33 patients with new enhanced mass lesion(s) on the initial post- radiotherapy MRI were screened, including 6 patients with tumor sub-totally removed, 4 patients without any functional imaging modality preformation and 1 patient lost to follow up. Finally, 22 patients who met the above criterial were included in this study.

In our daily clinical work, surgical operations or biopsies were preferred for patients suspicious of tumor recurrence under the following situations: *i*) Evidence supported by at least one functional imaging (MRP or PET); *ii*) Clinical symptoms could not be relieved by steroids or mannitol; *iii*) Family members' willingness and doctors' experience (especially when MRP and PET inspection results are inconsistent). In our study, for patients suspicious of treatment necrosis and were arranged for observation, if their image features got worse in the next follow-up and then received additional chemotherapy, these patients were excluded. Since this is a retrospective study, CTC detection results were not used as a consideration for subsequent treatment of patients.

Patients in our study were all from Beijing Tiantan hospital. This study was approved by the Medical Ethics Committee of Beijing Tiantan hospital (2017-2021) and written informed consent was obtained from all patients and healthy volunteers. To avoid bias, different experimental procedures in CTCs detection, including blood sample collection, enrichment, SE-iFISH and results interpretation were performed by different personnel. Results of DSC-MRP and 11C-MET-PET were analyzed by consensus interpretation of two board-certified neuro-radiologists who were blinded to the tissue diagnosis. The histological result of all specimens

was independently evaluated by three neuro-pathologists, with the diagnosis adhering to the WHO classification of CNS tumors. In our study, all patients underwent chest X-ray examination and blood tests routinely in our clinic, and those with abnormal results were not enrolled in our study.

2.2. CTC Subtraction enrichment and Immunostaining-FISH

The experimental procedures for CTC subtraction enrichment and immunostaining-FISH were mainly performed as previously described (*15,18*), with the procedure for CTCs images identification and collection improved. In CTC subtraction enrichment procedures, briefly, 7.5 mL peripheral blood was collected and centrifuged. Solutions above RBCs were collected and incubated with 150 μl of anti-WBC and endothelial cell immunomagnetic beads for 15 min and were centrifuged. The resulting pellet containing monolayer rare cells was thoroughly mixed with 100 μl cell fixative, followed by application to the formatted and coated CTC slide (Cytelligen). Next the immunostaining-FISH experimental procedure was performed. At first, samples on the coated CTC slides were subjected to Vysis Centromere Probe (CEP8) SpectrumOrange (Abbott Laboratories, Abbott Park, IL, USA) hybridization for 90 min using a S500 StatSpin ThermoBrite Slide Hybridization/Denaturation System (Abbott Molecular, Des Plaines, IL, USA), followed by incubation with Alexa Fluor 594 conjugated monoclonal anti-CD45, anti-GFAP (BD, USA). CTC is defined as $DAPI^+$, $CD45^-$, and heteroploidy CEP8 signal.

In our previous study, images of the CTCs were collected using a fluorescence microscope and visually identified by a pathologist. In this study, this procedure was improved so that images of the tumor cells were identified by a Zeiss Metafer-iFISH automated CTCs scanning system (Zeiss and MetaSystems, Germany, Cytelligen, USA).

2.3. DSC-MRP

MRI scans (n = 20) were performed using 3.0-T magnets (Trio, SIEMENS, Germany). DSC sequences were acquired using 5-mm slice thickness and 1.5-mm gap, and were obtained using gradient-echo echo-planar images (repetition time/echo time = 1400/32 ms, matrix 320 × 320, flip angle 90°, number of slices 19). A standard dose (0.2 mL/kg of body weight, maximum dose 20 mL) of gadopentetate dimeglumine (BEILU Pharmaceutical CO. LTD, Beijing, China) contrast was injected though a peripheral Angiocath (22 gauge) using 5 mL/s and immediately followed by a 20-ml saline flush at the same rate. Then multi-section image data were acquired every second for a total of 75 s, with the bolus contrast injection occurring after 10 s.

The axial DSC images were transferred to an offline commercially available workstation (MAGNETOM Trio. A Tim System, SIEMENS, Germany) and processed using commercially available software (NUMARIS/4, syngo MRB17, SIEMENS). To analyze the cerebral blood volume (CBV), ROI analysis for CBV was performed as follows: A single contrast section containing the maximum diameter of the enhancing lesion was selected, and an ROI was manually drawn around the entire enhancing lesion. Areas of hemorrhage, blood vessels, susceptibility artifacts, and cystic or necrotic change were excluded. Control ROI was placed over the contralateral normal-appearing white matter (CBV_{NL}) to calculate relative cerebral blood volume (rCBV). The rCBV measurements were recorded as CBV_{ROI} / CBV_{NL} as previously described (*16*). Negative enhancement integral perfusion maps were reconstructed using standard algorithms; blood vessels, cystic/necrotic changes, and areas of susceptibility from hemorrhage, bone, or air were excluded from the ROIs.

2.4. 11C-MET-PET

11C-MET-PET images (n = 17) were performed using a previously described methodology (*19*). Briefly, PET imaging was performed parallel to the orbit meatal line. A molded plastic facemask was used to restrict head motion. Images were obtained by intravenous bolus injection of 200-550 MBq of MET. All images were reconstructed using a conventional filtered back-projection algorithm, and were corrected for non-uniformity of detector response, dead time, random coincidences, and scattered radiation. After fusing the PET and contrast-enhanced T1-weighted images using commercial software (Xeleris 3 Functional Imaging Workstation, GE, USA), each ROI was manually placed on the lesion (including the pixel with the highest accumulation), using the contralateral region of the normal gray matter as a reference. The uptake lesion-to-normal tissue (L_{max}/N_{max}) ratios $rSUV_{max}$ were calculated from the maximum uptake of lesions and the reference area as visible in11C-MET-PET.

2.5. Statistical analysis

SPSS version 22.0 and MedCalc Version 16.8.4 (a statistical software package for biomedical research. including ROC curve analysis, method comparison and quality control tools, *https://www.medcalc.org/index.php*) were used for statistical analyses. Data were presented as the mean ± standard deviation (data obeyed normal distribution) or median with range (data that did not obey normal distribution). Comparisons between treatment necrosis and tumor recurrence groups were performed using Wilcoxon rank sum tests. Diagnosis efficacy of CTC, MPR and PET to differentiate treatment

necrosis from tumor recurrence were evaluated by ROC analysis. Optimal threshold values of CTCs count, rCBV and $rSUV_{max}$ were obtained by AUC analysis derived from ROC curves, to maximize the sum of sensitivity and specificity. In this study, $p < 0.05$ was considered statistically significant.

3. Results

3.1. Clinical characteristics, final diagnosis and grouping of these 22 patients

The authors identified 22 patients (12 males and 10 females, median age: 41 years, range from 31 to 55) who fulfilled the study criteria. All 22 patients received CTCs detection, and DSC-MRP and 11C-MET-PET were performed on 20 patients (90.9%) and 17 patients (77.3%) respectively. These 22 patients were divided into two groups, a tumor recurrence group (n = 10) and a treatment necrosis group (n = 12), according to evidence from the clinical course (n = 11) or histological confirmation (n = 11). Typical images of these two patient groups are shown in Figure 1.

In these two groups, no significant difference of the patients' baseline was observed. The mean age in the tumor recurrence and treatment necrosis group was 45.1 ± 5.28 and 39.8 ± 7.51 years respectively, and no significant difference (p = 0.073) was found. The sex distribution (male/female) of tumor recurrence and treatment necrosis group was 1.5:1 and 1:1 respectively, with no significant difference observed (p = 0.639). The ratio of high/low grade gliomas was 8:2 and 8:4 in tumor recurrence and treatment necrosis group respectively, which also revealed no significant difference (p = 0.481). The mean interval from radiotherapy was 12.2 ± 8.95 months (range: 3-29 months) in the tumor recurrence group and 13.9 ± 14.5 months (range: 3-37 months) in the treatment necrosis group, and no significance was observed (p = 0.748). Details on the patients' clinical characteristics are summarized in Table 1.

3.2. CTCs detection

Figure 2 A-E shows a CTC enriched from peripheral blood in one patient with GFAP positively expressed. A large strong polyploidy (≥ 5 copies) chromosome 8+ and CD45- CTC was observed, with GFAP positively expressed. WBCs surrounding CTC were diploid in chromosome 8, and stained positively for CD45. Figure

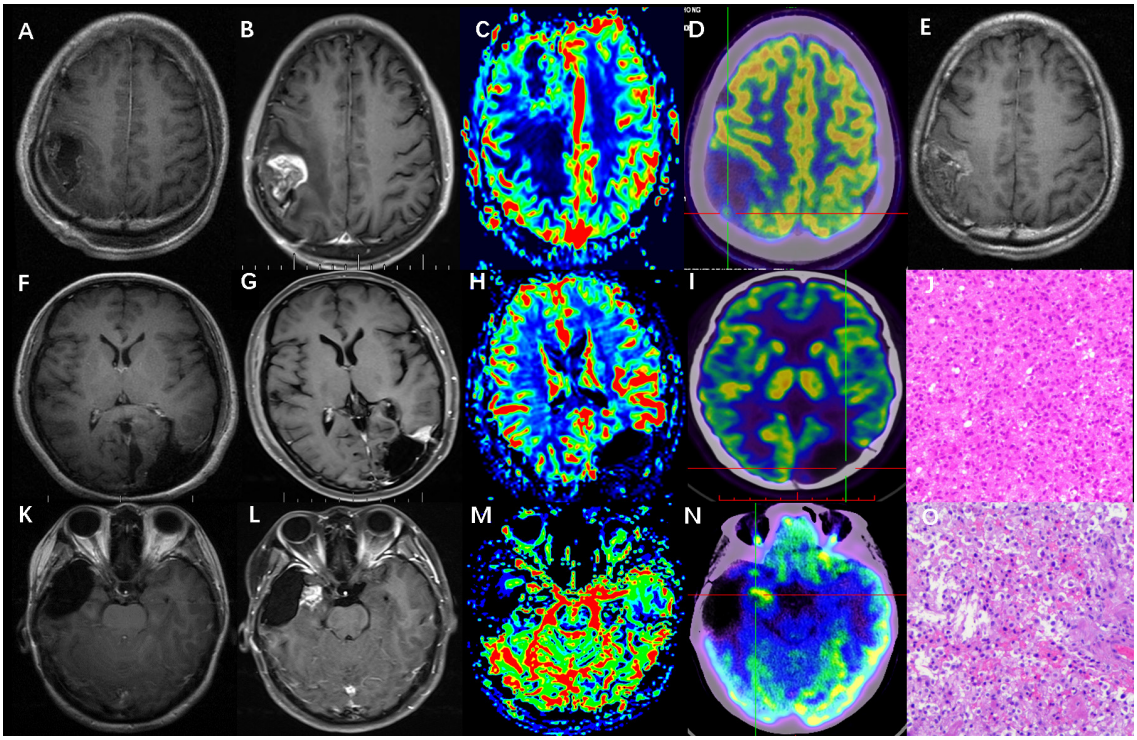

Figure 1. Typical images of 3 patients finally diagnosed as TN and TR. (A-E): 1 patient (No. 3 in table 1, CTC counts was 0) was finally diagnosed as treatment necrosis. (A) Enhancing MR image after gross total resection. **(B)** Enhancing MR image after completion of first radio-chemotherapy. **(C)** Simultaneous DSC-MRP showed hypoperfusion in the enhancing lesion. **(D)** Simultaneous 11C-MET-PET showed hypo metabolism in the enhancing lesion. **(E)** Enhancing MR image after 9 months' follow-up period, the enhancing lesion was significantly decreased. **(F-O)**:1 patient (No. 4 in table 1, CTC counts was 3) was finally diagnosed as tumor recurrence **(F-J)** and 1 patient (No. 12 in table 1, CTC counts was 1) was diagnosed as treatment necrosis **(K-O)** respectively. **(F, K)** Enhancing MR image after gross total resection. **(G, L)** Enhancing MR image after completion of first radio-chemotherapy. **(H, M)** Simultaneous DSC-MRP showed hyperperfusion in the enhancing lesion. **(I, N)** Simultaneous 11C-MET-PET showed hyper metabolism in the enhancing lesion. **(J, O)** Pathological findings of tumor recurrence **(J)** and treatment necrosis **(O)** after the subsequent surgery (HE, 10×10).

Table 1. Characteristics and diagnosis of 22 patients who underwent CTCs detection, DSC-MRP and 11C-MET-PET

No.	Age (years)/Sex	Primary diagnosis	Adjuvant Thera-py/Interval from RT(month)	KPS	CTC counts	DSC	MEG-PET	TR or TN by Cl/ Pa (Bio/Res)
						$rCBV_{ROI}$	$rSUV_{max}$	
1	55/F	OA	TMZ/17	90	0	0.66	no exam	TN(Cl)
2	45/M	GBM	TMZ/13	90	2	2.38	3.00	TR(Pa, Res)
3	41/M	GBM	TMZ/3	90	0	0.52	0.76	TN(Cl)
4	45/F	GBM	TMZ/6	70	3	2.27	3.83	TR(Pa. Res)
5	41/F	GBM	TMZ/7	90	3	2.07	3.80	TR(Pa, Res)
6	31/M	AOA	TMZ/4	80	0	2.67	1.82	TN(Cl)
7	41/M	OA	None/21	80	5	2.43	3.70	TR(Pa, Res)
8	53/M	AO	TMZ/3	90	0	0.85	1.71	TN(Cl)
9	46/F	AA	TMZ/29	80	8	0.65	1.93	TR(Pa, Res)
10	40/M	A	None/20	90	5	2.01	4.00	TR(Pa, Res)
11	40/F	GBM	TMZ/37	90	0	0.61	3.94	TN(Cl)
12	34/F	AA	TMZ/10	90	1	2.44	3.29	TN(Pa, Res)
13	31/F	AOA	TMZ/21	90	9	no exam	2.20	TN(Cl)
14	36/M	A	None/4	90	0	0.48	no exam	TN(Cl)
15	41/M	OA	AVM/7	90	1	0.57	no exam	TN(Cl)
16	39/F	OA	None/47	90	1	0.44	no exam	TN(Cl)
17	39/M	AA	None/11	90	1	0.48	2.50	TN(Cl)
18	47/M	GBM	TMZ/3	80	10	2.18	no exam	TR(Pa, Res)
19	37/F	GBM	TMZ/3	90	0	no exam	2.61	TN(Cl)
20	40/M	GBM	TMZ/15	70	8	2.58	4.80	TR(Pa, Bio)
21	55/F	GBM	TMZ/6	70	12	0.86	2.43	TR(Pa, Bio)
22	53/M	GBM	TMZ/5	80	5	0.55	5.70	TR(Pa, Bio)

Abbreviations: A, astrocytoma; AA, anaplastic astrocytoma; AO, anaplastic oligodendroglioma; AOA, anaplastic oligoastrocytoma; AVM, nimustine, vincristine and methotrexate; Bio, biopsy; Cl, clinically diagnosed; GBM, glioblastoma multiforme; KPS, Karnofsky performance scale; OA, oligoastrocytoma; Pa, pathologically diagnosed; Res, surgical resection; RT, radiotherapy; TMZ, temozolomide; TN, treatment necrosis; TR, tumor recurrence.

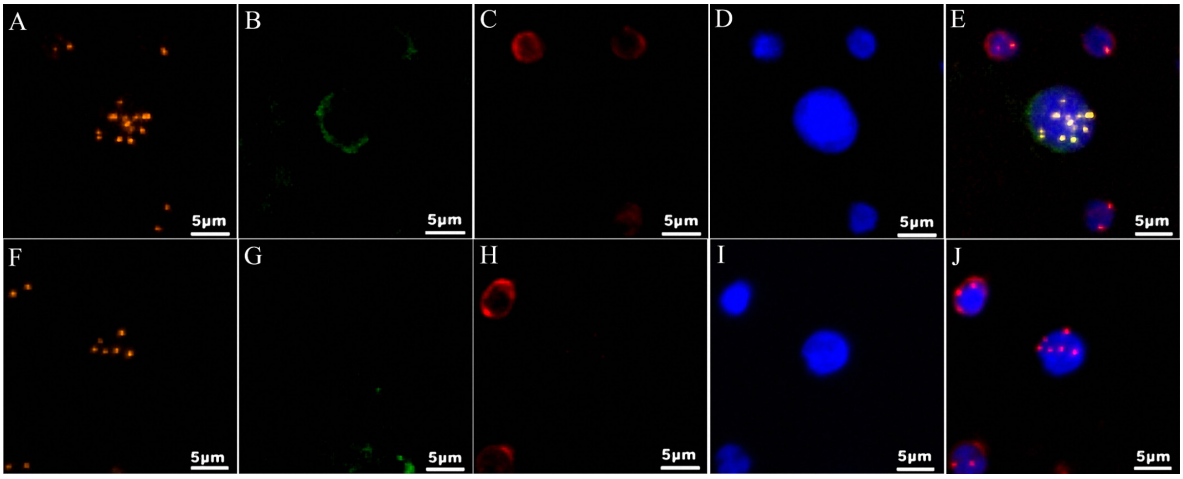

Figure 2. Characteristics of a CTC with GFAP expressed in the peripheral blood of one glioma patient. (A-D) CTC observed was $FISH^+$ (polyploidy chromosome 8, orange, A) /$GFAP^+$(green, B) / $CD45^-$ (red, C) and $DAPI^+$ (blue, D). **(E)** Four images emerged. WBCs surrounding CTC were diploid in chromosome 8, and stained positively for CD45, without GFAP expressed. **(F-J)** Image of a CTC without GFAP expressed in another patient.

2 F-J shows 1 CTC detected with GFAP negative expressed from the same patient. In our study, CTCs were found with GFAP positively expressed in only 1 patient (total 5 cells, 1 cell with GFAP positively expressed and 4 cells with GFAP negatively expressed), similar to our previous results.

No CTC was detected in 20 healthy volunteers. In 22 patients, results of CTCs detection revealed that the mean CTCs count were significantly higher in tumor recurrence group (6.10 ± 3.28), compared to treatment necrosis group (1.08 ± 2.54, $p < 0.001$), as shown in Figure 3. An optimized CTCs count threshold of 2 had 100% sensitivity and 91.2% specificity with AUC = 0.933 to declare tumor recurrence. ROC curves are shown in Figure 4A; the diagnostic results of ROC are shown in Table 2.

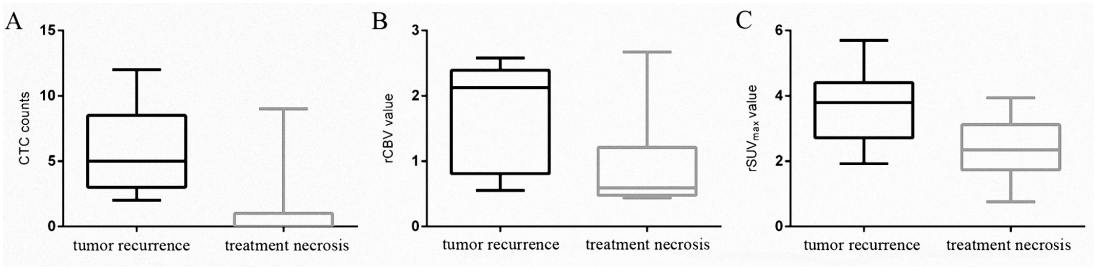

Figure 3. Box-and-whisker plots for CTCs counts, rCBV value and $rSUV_{max}$ value in TR (tumor recurrence) and TN (treatment necrosis) group.

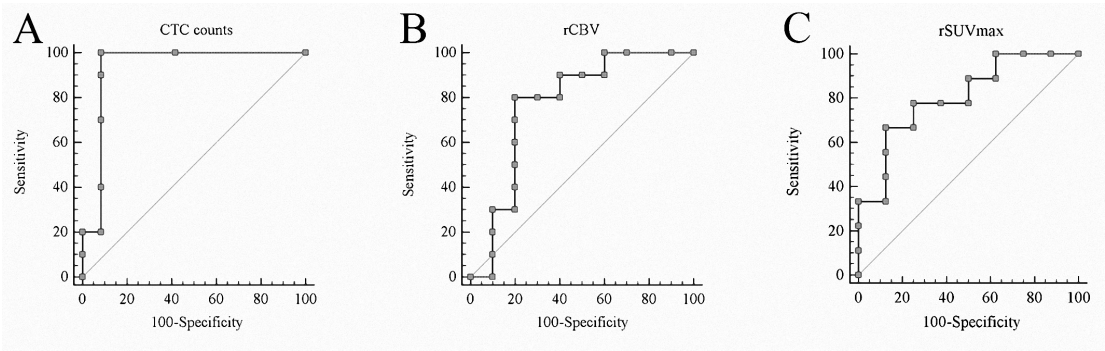

Figure 4. Roc curve associated with CTCs detection, DSC-MRP and 11C-MET-PET to differentiate tumor recurrence from treatment necrosis.

Table 2. Comparison of diagnostic results of CTCs detection, DSC-MRP, 11C-MET-PET in diagnosis of tumor recurrence in 22 patients

variables	CTCs counts (n = 22)	rCBV (n = 20)	$rSUV_{max}$ (n = 17)
Sensitivity (%)	100. 0	80. 0	66.7
Specificity (%)	91.7	80. 0	87.5
Positive predictive value (%)	90.9	80. 0	85.7
Negative predictive value (%)	100. 0	80. 0	70. 0
Accuracy (%)	95.5	80. 0	76.5

3.3. DSC-MRP

Results of DSC-MRP showed that the mean $rCBV_{ROI}$ was higher in tumor recurrence group (1.80 ± 0.79), compared to treatment necrosis group (0.96 ± 0.82, p = 0.031). An optimized $rCBV_{ROI}$ threshold of > 0.85 had 80% sensitivity and 80% specificity with AUC = 0.770 to declare tumor. ROC curves are shown in Figure 4B; the diagnostic results of ROC are shown in Table 2.

3.4. 11C-MET-PET

Results of 11C-MET-PET showed that the mean $rSUV_{max}$ was higher in tumor recurrence group (3.69 ± 1.15), compared to treatment necrosis group (2.35 ± 0.98, p = 0.022). An optimized $rSUV_{max}$ threshold of > 3.29 had 66.7% sensitivity and 87.5% specificity with AUC = 0.806 to declare tumor. ROC curves are shown in Figure 4C; and the diagnostic results of ROC are shown in Table 2.

3.5. CTCs detection could predict tumor recurrence in one of these 22 patients

A 40-year-old male suffering from a severe headache was admitted to our hospital and MR imaging showed an enhanced mass lesion in his left temporal lobe. The patient received surgical resection and was diagnosed with glioblastoma multiform (GBM) through histology. The tumors were completely removed and no enhancing lesion was observed on MRI imaging after the operation was complete (Figure 5A). After surgery, the patient was arranged to undergo radio-chemotherapy, with a total radiation dose of 6000 cGy to the extended local zone using the hyper-fractionated method. Follow-up MR imaging revealed a new enhancing lesion in the left hippocampus six months later (Figure 5B). Although a chemotherapy plan was suggested, the patient did not experience any clinical discomfort, and refused to receive any anti-tumor treatment. During the follow-up periods no obvious symptoms were detected, and

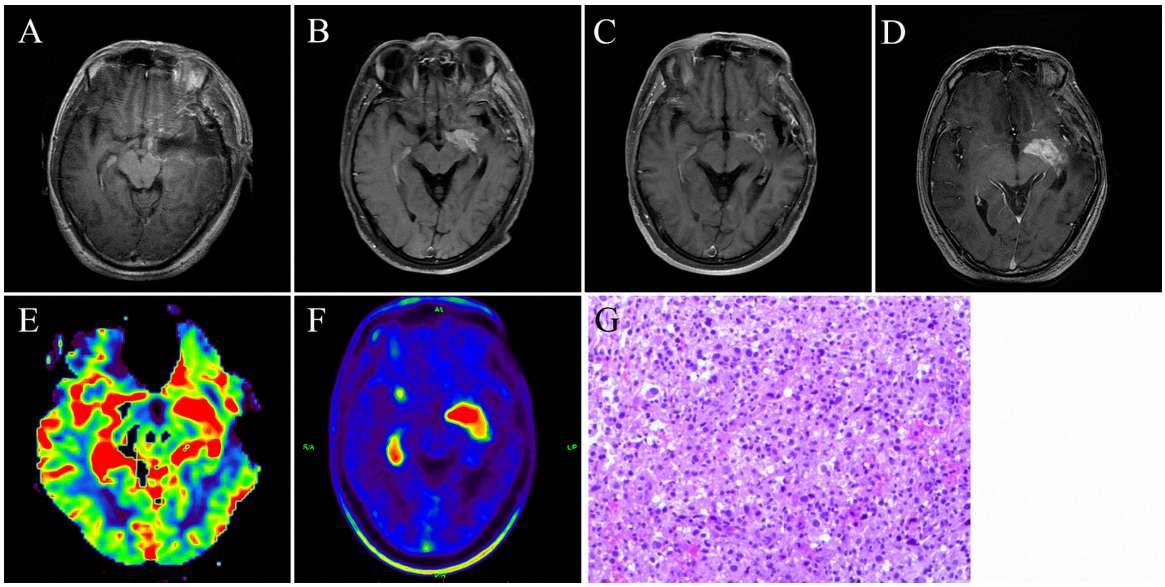

Figure 5. An illustrative case indicating the predictive role of CTCs detection in tumor recurrence. (A-D) Contrast axial T1-weighted image: **(A)** After gross total resection, there is a surgical cavity without enhancement. **(B)** After completion of radio-chemotherapy, there is a new enhancing mass lesion on the initial post- radiotherapy MRI. **(C)** Nine months later, MR imaging revealed that the enhancing lesion decreased. **(D)** Three months later, MR imaging showed that the enhancing lesion finally significantly increased. **(E)** Simultaneous DSC-MRP showed hyper perfusion in the enhancing lesion. **(F)** Simultaneous 11C-MET-PET showed hyper metabolism in the enhancing lesion. **(G)** Pathological findings of tumor recurrence of GBM after biopsy (HE, 10×10).

nine months later, the next MR imaging revealed that the enhancing lesion had significantly decreased (Figure 5C). This development suggested a diagnosis of treatment necrosis. To our surprise however, four CTCs were detected in his blood, which was higher than our previous experience in the treatment necrosis group. Given that no clinical symptoms were observed with better features on MRI imaging, the patient did not receive any anti-tumor treatment but was asked to follow up. Unfortunately, three months later, the patient was once again admitted to our hospital for memory loss and a continuous headache. MR imaging showed that the enhancing lesion had significantly increased (Figure 5D). Simultaneous DSC-MRP and 11C-MET-PET demonstrated the higher rCBV (Figure 5E) and $rSUV_{max}$ (Figure 5F) in the enhancing lesion, and CTCs detection showed that the CTCs counts increased to eight (patient No. 20 in Table 1). A biopsy was performed and histological examination resulted in a diagnosis of tumor recurrence (Figure 5G).

4. Discussion

Numerous studies have investigated the roles of different functional imaging modalities in differentiating treatment necrosis from tumor recurrence (*6,20,21*). In 2013, Komotar conducted a systematic review to explore the value of a variety of functional imaging modalities, including MRS, ASL MRI (arterial spin-labeled MR imaging), DSC-MRP, CTP, SPECT, 18F-FDG-PET and 11C-MET-PET, in the diagnosis of treatment necrosis and tumor recurrence, but most of the results were disappointing because a high sensitivity and specificity could not be achieved concurrently in one modality. Of the explored modalities, SPECT has the potential to be the best modality, but low spatial resolution and tracer uptake in normal tissues of the choroid plexus and pituitary gland have limited its clinical application (*6*). More importantly, reported results achieved by the same modality are sometimes inconsistent. For example, Tsuyuguchi reported that the sensitivity and specificity of 11C-MET-PET in differentiating treatment necrosis from tumor recurrence were 100% and 60%, respectively (*22*). While Kim's study, in contrast, reported that the sensitivity and specificity of 11C-MET-PET were 75% and 100%, respectively (*19*). Concerning another commonly used parameter, rCBV in MRP, the diagnostic efficacy in differentiating treatment necrosis from tumor recurrence is also quite variable. Sugahara and Huang reported the sensitivity of rCBV for detecting tumor recurrence was 50% and 56%, respectively (*23,24*), while Matsusue and Mitsuya reported sensitivity of 90% and 100% respectively *(25,26)*. A variety of reasons could explain this phenomenon: the inherent limitation of each functional imaging modality, the usual overlap imaging features of the two lesions, and the subjective bias involved in data analysis procedures. Thus far, insufficient and inconsistent diagnostic efficacy, together with high operational costs and low insurance coverage, has limited their clinical application, which needs further evaluation to establish their reliability and robustness in differentiating these two lesions.

In our study, 22 patients were divided into tumor

recurrence group (n = 10) and treatment necrosis group (n = 12), according to evidence from the clinical course (n = 11) or histological confirmation (n = 11). Only half of these patients' diagnoses were proven by histological confirmation, because treatment necrosis was mostly proven by clinical course (11 patients), with only 1 patient proven by histological result after surgery. This is mainly due to the very strict and complex surgical indications for these patients (described in material and methods section below); but even to do this, there was still one patient who was operated on and diagnosed with treatment necrosis finally, suffering left hemiplegia after. Another reason is that although biops were performed in many neurosurgery centers, in our institute this was not widely used.

It has been demonstrated in recent years that CTCs detection in the blood *via* so-called "liquid biopsies" has an important clinical translational value for its direct biological reflection of tumor microenvironments, without the need for repeated neurosurgical procedures with inherent risk of patient morbidity (*8-10,27-30*). But related studies of CTCs application in CNS malignancies are quite limited. In the recent three years, a few studies have successfully isolated CTCs in patients of both primary and recurrent GBM and diffuse glioma, which initiated related studies in brain gliomas (*12-14*). In 2014, Dorsey noticed that sequential CTCs counts increased and decreased in 2 patients later diagnosed with "tumor recurrence" and "Pseudo recurrence", respectively. Our previous study further confirmed that CTCs could be detected in all 7 common subtypes of primary brain gliomas, and to some extent, has superiority to MRP in identification of treatment necrosis or tumor recurrence in 5 patients (*15*). Due to the quite distinct tumor microenvironment of treatment necrosis and tumor recurrence, we postulated that CTCs counts of these 2 lesions could be significantly different, which should be proven by in a systematic study with a larger sample size and include common functional imaging modalities for comparison purposes.

Since the detection of CTCs in the blood of glioma patients was initiated recently, the technology adopted in each institution was different. The earliest method used to find CTCs was based on the detection of tumor cell surface specific markers such as GFAP. Muller *et al.* identified CTCs in blood from 29 of 141 (20.6%) GBM patients by immunostaining of GFAP and stated that CTCs are an "intrinsic property" of GBM biology (*14*). However, GFAP expression is not totally restricted to glial cells (*31,32*), and more importantly, some tumor cell markers lost their expression in blood. For example, it was reported that CK18, the dual epithelial marker and tumor biomarker, was positive in only 14% of lung and 24% of esophageal CTCs, respectively (*18*). In this study, the methodology we applied for CTCs detection was similar to our previous study, which was initially reported by Ge *et al.* in 2015, who has first detected glioma tumor cells in CSF, based on polyploidy of chromosome 8 examination by CEP8-FISH (*18*). We choose this protocol because compared to surface markers, aneuploidy, or abnormal chromosome content, could be the more common and stable marker of human solid tumors, for its characteristics that contribute to, or even drive, tumor development (*33*). Numerous studies have demonstrated the aneuploidy chromosome in many solid tumors; concerning brain glioma, it is also reported that polysomy of chromosome 8 could be found in CGH array results of 172 patients with GBM in a TCGA dataset, with a highest frequency of about 30-40% in one subgroup (*34*). In our previous study, we also demonstrated that chromosome 8 polyploidy cells generally existed in glioma specimens (*15*), providing the feasibility of CTCs detection based on aneuploidy chromosome.

Different from our previous study with CTCs detection in brain gliomas not treated, CTCs detection were performed in 10 recurrent gliomas after radiotherapy, and results showed that the CTC incidence was 100%, higher than our previous results (with CTC incidence of 77%). We speculated that the high incidence could be mainly due to the blood-brain barrier disruption after radio-chemo therapy (this is also the mechanism of the enhancing features of MRI), which could facilitate tumor cells entering the circulation. However, immunostaining results showed that only one patient was found with GFAP positive expressed, which was consistent with our previous results (*15*). Although the mechanisms of how GFAP expression was lost in the blood is still unknown, the present study has demonstrated the higher feasibility of CTCs detection in gliomas after radiotherapy, which could yield great potential for brain gliomas monitoring and treatment planning.

In our results, the sensitivity and specificity of rCBV and 11C-MET-PET in differentiating treatment necrosis from tumor recurrence were consistent with the findings of previous studies. CTCs counts were significantly different in the treatment necrosis and tumor recurrence groups, and by setting a cut-off value of 2, the ROC curve results showed that CTCs detection had a superior diagnostic efficacy compared to DSC-MRP and 11C-MET-PET. The different CTCs counts in treatment necrosis and tumor recurrence groups did meet our expectations because it is reasonable to suppose that the tumor burdens of these two lesions are quite different. However, the result obtained using the cut-off value of 2, rather than a cut-off of 0, was quite surprising. In this study, tumors were gross totally removed in all patients, and those patients with sub-totally removed tumors were not included, due to the unclear assumption about the difference in CTCs counts between recurrent tumor and residual tumors after surgery. Our results showed that even with visible surgical total resection on MRI imaging, CTCs were

still positive in four patients (with CTCs counts of 1). The results were consistent with the phenomenon that a new contrast-enhancing lesion observed *via* imaging is neither solely necrotic tissue nor tumor, but rather a mixture of both lesions. The present results demonstrate an advantage of CTCs detection in effective diagnosis of treatment necrosis and tumor recurrence, which is largely due to its direct reflection of the brain tumor environment after combined clinical treatment, rather than the indirect manifestation and computational results used by imaging modalities.

Beyond its application in differentiating treatment necrosis from tumor recurrence, our results could have additional illuminating indications. At first we wonder whether CTCs counts could have some prognostic effects in brain gliomas recurrence. In our study, we noticed that one patient (case 20) had 4 CTCs, but the enhancing lesion on MRI imaging decreased compared to the first enhancing lesion after radiotherapy. However, the enhancing lesion increased subsequently and tumor recurrence was finally confirmed three months later. The most likely explanation of this phenomenon is the usual overlap features of treatment necrosis and tumor recurrence on imaging, and the different evolution of treatment necrosis and tumor recurrence in the same enhancing lesion. Since several studies have shown a predictive role of CTCs count in tumor recurrence in other non-CNS tumors (*10,35,36*), we supposed that even in the same treatment necrosis group, those patients with different CTCs counts could have different prognoses, which would be proven during the next follow-up. Furthermore, we believe that the essential goal of differentiating treatment necrosis from tumor recurrence is not the "diagnosis" itself, but developing a "treatment plan" for the patient. Therefore, whether sequential CTCs detection in those patients should be performed and whether the treatment should be individually modified according to the sequential CTCs count still needs further study. Since this is the first step toward investigating the translational value of CTCs detection in brain gliomas, these interesting questions might be even more meaningful than the diagnostic result itself.

To date, histological confirmation is still the gold standard for differentiating treatment necrosis from tumor recurrence, but its sampling error and observer variability limitations make it an imperfect method. Furthermore, even in the case of treatment-related necrosis, areas with tumor cells are often present between large areas with necrosis, and it is very difficult to verify whether these tumor cells are still viable (*37*). Compared to histology, CTCs detection could reflect the invisible tumor status directly, and its continuous value could provide more information than the very rigid 2-group division used in histology. Besides its accurate diagnostic efficacy, CTCs detection has other advantages over imaging modalities. First, only a 7.5 mL blood sample was collected, and the experimental time requirement for patients was much shorter. Second, in our study, CTCs were identified by an automated CTC scanning system, which made our results more objective and reproducible. Lastly, compared to most functional imaging modalities, CTCs count is an absolute number, not a relative ratio, which could make the monitoring process more accessible. Considering the above advantages, we believe, as a new biomarker that directly comes from brain tumors (visible or invisible on imaging), CTCs detection could be a reliable tool for differentiating treatment necrosis from tumor recurrence, which both have very different tumor burdens.

Additionally, in our study, some patients' intervals from radiation therapy had a value of within 6 months. In a popular opinion, for the gliomas after radiation therapy, the radionecrosis often occurs in the late stage of radiation damage, which is over 6 months' after radiation therapy, and pseudo progression often occurs within 3 months after radiation therapy. Therefore, it is relatively easy to cause conceptual confusion of the generalized term "treatment necrosis". In fact, we initially wanted to change "treatment necrosis" to "treatment response" or "treatment effect". After serious consideration, we decided to proceed with the term "treatment necrosis." The underlying reasons are: on the one hand, compared with "treatment response" and "treatment effect" – which are too wide in scope – "treatment necrosis" describes our research purpose more accurately; on the other hand, from a pathophysiological point of view, according to certain studies, pseudo progression can be broadly considered as a period of "acute or sub-acute necrosis" with symptoms that are usually recoverable. Radiation necrosis, in this regard, can be broadly interpreted as "the late stage of necrosis" with a predominantly irreversible course of disease (*37*). Therefore, considering the above mentioned reasons, we preferred using "treatment necrosis" (not radiation necrosis).

There are, inevitably, some shortcomings in our study, including the relatively small size of the final analysis cohort and the retrospective design. Our study only focused on the situation after the first radiotherapy, and did not follow up the CTC examination in most patients and compare it with the clinical course. Therefore, the diagnosis of CTC cannot be clarified after multiple treatments in this study. Most of these patients did not receive continuous CTC detection, and since this is not a prospective study, the prognostic potential of CTCs detection in these cases cannot be disclosed at present. At last, patients with subtotal and partial resection of tumors are not included, and this may account for a large part of clinical work. A prospective, larger sample size study would provide more information about the application value of CTCs detection. These efforts are currently being pursued in our ongoing studies.

Funding: This study was supported by Natural Science Foundation of Zhejiang Province (No. LY19H160035), and Zhejiang Province Public Welfare Technology Application Research Project (No. LGF20G030011), and National Natural Science Foundation of China (81771309).

Conflict of Interest: The authors have no conflicts of interest to disclose.

References

1. Stupp R, Mason WP, Van Den Bent MJ, *et al.* Radiotherapy plus concomitant and adjuvant temozolomide for glioblastoma. N Engl J Med. 2005; 352:987-996.
2. Peca C, Pacelli R, Elefante A, De Caro MDB, Vergara P, Mariniello G, Giamundo A, Maiuri F. Early clinical and neuroradiological worsening after radiotherapy and concomitant temozolomide in patients with glioblastoma: tumour progression or radionecrosis? Clin Neurol Neurosurg. 2009; 111:331-334.
3. Wen PY, Macdonald DR, Reardon DA, *et al.* Updated response assessment criteria for high-grade gliomas: response assessment in neuro-oncology working group. J Clin Oncol. 2010; 28:1963-1972.
4. Melguizo-Gavilanes I, Bruner JM, Guha-Thakurta N, Hess KR, Puduvalli VK. Characterization of pseudoprogression in patients with glioblastoma: is histology the gold standard? J Neurooncol. 2015; 123:141-150.
5. Strauss SB, Meng A, Ebani EJ, Chiang GC. Imaging glioblastoma posttreatment: progression, pseudoprogression, pseudoresponse, radiation necrosis. Neuroimaging Clin N Am. 2021; 31:103-120.
6. Shah AH, Snelling B, Bregy A, Patel PR, Tememe D, Bhatia R, Sklar E, Komotar RJ. Discriminating radiation necrosis from tumor progression in gliomas: a systematic review what is the best imaging modality? J Neurooncol. 2013; 112:141-152.
7. Verma N, Cowperthwaite MC, Burnett MG, Markey MK. Differentiating tumor recurrence from treatment necrosis: a review of neuro-oncologic imaging strategies. Neuro Oncol. 2013; 15:515-534.
8. Riethdorf S, Müller V, Zhang L, *et al.* Detection and HER2 expression of circulating tumor cells: prospective monitoring in breast cancer patients treated in the neoadjuvant GeparQuattro trial. Clin Cancer Res. 2010; 16:2634-2645.
9. Pachmann K, Camara O, Kavallaris A, Krauspe S, Malarski N, Gajda M, Kroll T, Jörke C, Hammer U, Altendorf-Hofmann A, Rabenstein C, Pachmann U, Runnebaum I, Höffken K. Monitoring the response of circulating epithelial tumor cells to adjuvant chemotherapy in breast cancer allows detection of patients at risk of early relapse. J Clin Oncol. 2008; 26:1208-1215.
10. Cristofanilli M, Budd GT, Ellis MJ, Stopeck A, Matera J, Miller MC, Reuben JM, Doyle GV, Allard WJ, Terstappen LW, Hayes DF. Circulating tumor cells, disease progression, and survival in metastatic breast cancer. N Engl J Med. 2004; 351:781-791.
11. Terheggen HG, Müller W. Extracerebrospinal metastases in glioblastoma. Eur J Pediatr. 1977; 124:155-164.
12. Sullivan JP, Nahed BV, Madden MW, *et al.* Brain tumor cells in circulation are enriched for mesenchymal gene expression. Cancer Discov. 2014; 4:1299-1309.
13. MacArthur KM, Kao GD, Chandrasekaran S, Alonso-Basanta M, Chapman C, Lustig RA, Wileyto EP, Hahn SM, Dorsey JF. Detection of brain tumor cells in the peripheral blood by a telomerase promoter-based assay. Cancer Res. 2014; 74:2152-2159.
14. Müller C, Holtschmidt J, Auer M, *et al.* Hematogenous dissemination of glioblastoma multiforme. Sci Transl Med. 2014; 6:247ra101.
15. Gao F, Cui Y, Jiang H, Sui D, Wang Y, Jiang Z, Zhao J, Lin S. Circulating tumor cell is a common property of brain glioma and promotes the monitoring system. Oncotarget. 2016; 7:71330-71340.
16. Prager AJ, Martinez N, Beal K, Omuro A, Zhang Z, Young RJ. Diffusion and perfusion MRI to differentiate treatment-related changes including pseudoprogression from recurrent tumors in high-grade gliomas with histopathologic evidence. AJNR Am J Neuroradiol. 2015; 36:877-885.
17. Minniti G, Clarke E, Lanzetta G, Osti MF, Trasimeni G, Bozzao A, Romano A, Enrici RM. Stereotactic radiosurgery for brain metastases: analysis of outcome and risk of brain radionecrosis. Radiat Oncol. 2011; 6:48.
18. Ge F, Zhang H, Wang DD, Li L, Lin PP. Enhanced detection and comprehensive in situ phenotypic characterization of circulating and disseminated heteroploid epithelial and glioma tumor cells. Oncotarget. 2015; 6:27049-27064.
19. Kim YH, Oh SW, Lim YJ, Park CK, Lee SH, Kang KW, Jung HW, Chang KH. Differentiating radiation necrosis from tumor recurrence in high-grade gliomas: assessing the efficacy of 18 F-FDG PET, 11 C-methionine PET and perfusion MRI. Clin Neurol Neurosurg. 2010; 112:758-765.
20. Alexiou GA, Tsiouris S, Kyritsis AP, Voulgaris S, Argyropoulou MI, Fotopoulos AD. Glioma recurrence versus radiation necrosis: accuracy of current imaging modalities. J Neurooncol. 2009; 95:1-11.
21. Caroline I, Rosenthal MA. Imaging modalities in high-grade gliomas: pseudoprogression, recurrence, or necrosis? J Clin Neurosci. 2012; 19:633-637.
22. Tsuyuguchi N, Takami T, Sunada I, Iwai Y, Yamanaka K, Tanaka K, Nishikawa M, Ohata K, Torii K, Morino M, Nishio A, Hara M. Methionine positron emission tomography for differentiation of recurrent brain tumor and radiation necrosis after stereotactic radiosurgery – in malignant glioma. Ann Nucl Med. 2004; 18:291-296.
23. Sugahara T, Korogi Y, Tomiguchi S, Shigematsu Y, Ikushima I, Kira T, Liang L, Ushio Y, Takahashi M. Posttherapeutic intraaxial brain tumor: the value of perfusion-sensitive contrast-enhanced MR imaging for differentiating tumor recurrence from nonneoplastic contrast-enhancing tissue. AJNR Am J Neuroradiol. 2000; 21:901-909.
24. Huang J, Wang AM, Shetty A, Maitz AH, Yan D, Doyle D, Richey K, Park S, Pieper DR, Chen PY, Grills IS. Differentiation between intra-axial metastatic tumor progression and radiation injury following fractionated radiation therapy or stereotactic radiosurgery using MR spectroscopy, perfusion MR imaging or volume progression modeling. Magn Reson Imaging. 2011; 29:993-1001.
25. Matsusue E, Fink JR, Rockhill JK, Ogawa T, Maravilla KR. Distinction between glioma progression and post-radiation change by combined physiologic MR imaging.

Neuroradiology. 2010; 52:297-306.
26. Mitsuya K, Nakasu Y, Horiguchi S, Harada H, Nishimura T, Bando E, Okawa H, Furukawa Y, Hirai T, Endo M. Perfusion weighted magnetic resonance imaging to distinguish the recurrence of metastatic brain tumors from radiation necrosis after stereotactic radiosurgery. J Neurooncol. 2010; 99:81-88.
27. Pantel K, Brakenhoff RH, Brandt B. Detection, clinical relevance and specific biological properties of disseminating tumour cells. Nat Rev Cancer. 2008; 8:329-340.
28. Pierga JY, Bidard FC, Mathiot C, Brain E, Delaloge S, Giachetti S, de Cremoux P, Salmon R, Vincent-Salomon A, Marty M. Circulating tumor cell detection predicts early metastatic relapse after neoadjuvant chemotherapy in large operable and locally advanced breast cancer in a phase II randomized trial. Clin Cancer Res. 2008; 14:7004-7010.
29. Maheswaran S, Haber DA. Circulating tumor cells: a window into cancer biology and metastasis. Curr Opin Genet Dev. 2010; 20:96-99.
30. Pantel K, Alix-Panabières C. Circulating tumour cells in cancer patients: challenges and perspectives. Trends Mol Med. 2010; 16:398-406.
31. Danielyan L, Tolstonog G, Traub P, Salvetter J, Gleiter CH, Reisig D, Gebhardt R, Buniatian GH. Colocalization of glial fibrillary acidic protein, metallothionein, and MHC II in human, rat, NOD/SCID, and nude mouse skin keratinocytes and fibroblasts. J Invest Dermatol. 2007; 127:555-563.
32. Lim MC, Maubach G, Zhuo L. Glial fibrillary acidic protein splice variants in hepatic stellate cells – expression and regulation. Mol Cells. 2008; 25:376-384.
33. Kops GJ, Weaver BA, Cleveland DW. On the road to cancer: aneuploidy and the mitotic checkpoint. Nat Rev Cancer. 2005; 5:773-785.
34. Kim YW, Koul D, Kim SH, Lucio-Eterovic AK, Freire PR, Yao J, Wang J, Almeida JS, Aldape K, Yung WK. Identification of prognostic gene signatures of glioblastoma: a study based on TCGA data analysis. Neuro Oncol. 2013; 15:829-839.
35. Mejean A, Vona G, Nalpas B, Damotte D, Brousse N, Chretien Y, Dufour B, Lacour B, Bréchot C, Paterlini-Bréchot P. Detection of circulating prostate derived cells in patients with prostate adenocarcinoma is an independent risk factor for tumor recurrence. J Urol. 2000; 163:2022-2029.
36. Morgan TM, Lange PH, Porter MP, Lin DW, Ellis WJ, Gallaher IS, Vessella RL. Disseminated tumor cells in prostate cancer patients after radical prostatectomy and without evidence of disease predicts biochemical recurrence. Clin Cancer Res. 2009; 15:677-683.
37. Brandsma D, Stalpers L, Taal W, Sminia P, van den Bent MJ. Clinical features, mechanisms, and management of pseudoprogression in malignant gliomas. Lancet Oncol. 2008; 9:453-461.

Received January 10, 2021; Revised April 2, 2021; Accepted April 17, 2021.

[§]These authors contributed equally to this work.

*Address correspondence to:
Song Lin, Department of Neurosurgery, Beijing Tiantan Hospital, Capital Medical University; China National Clinical Research Center for Neurological Diseases, Beijing 100160, China.
E-mail: linsong2005@126.com

Released online in J-STAGE as advance publication April 29, 2021.